

Impact of deposition pressure and two-step growth technique on the photoresponsivity enhancement of polycrystalline BaSi₂ films formed by sputtering

Satoshi Matsuno¹, Taira Nemoto¹, Masami Mesuda², Hideto Kuramochi², Kaoru Toko¹, Takashi Suemasu¹

¹Institute of Applied Physics, University of Tsukuba, Ibaraki 305-8573, Japan

²Tosoh Corporation, Advanced Materials Research Laboratory, Kanagawa 252-1123, Japan

We investigate the influence of deposition pressure in the range 0.25–1.0 Pa on the photoresponsivity of 200-nm-thick BaSi₂ films grown by sputtering at 600 °C. BaSi₂ films formed at 0.8 Pa exhibit a high photoresponsivity. The deposited Ba-to-Si atomic ratio depends significantly on the sputtering pressure. That's why the pressure influences the photoresponsivity. BaSi₂ films grown by a two-step growth technique show much higher photoresponsivity almost equivalent to those grown by molecular beam epitaxy. The photoresponsivity reaches 0.75 A/W at 2.0 eV at a bias voltage of 0.5 V applied between the top and bottom electrode.

Wafer-based silicon (Si) solar cells dominate the market share, and their conversion efficiency (η) has exceeded 26%.¹⁾ The achieved η is already close to the theoretical limit.²⁾ Under these circumstances, various thin-film solar cell materials have been studied.³⁻⁶⁾ Among these materials, we have paid special attention to semiconducting barium disilicide (BaSi_2). Solar cell materials should be safe, stable, and earth-abundant like Si. In addition, a large absorption coefficient (α), a suitable band gap, and superior minority-carrier properties are important for solar cell materials to achieve a high η . BaSi_2 has all these properties.^{7,8)} It has a band gap of 1.3 eV,⁹⁾ a large α of $3 \times 10^4 \text{ cm}^{-1}$ at 1.5 eV,¹⁰⁻¹²⁾ inactive grain boundaries,¹³⁾ and a large minority-carrier lifetime ($\tau \sim 10 \text{ }\mu\text{s}$).^{14,15)} We have achieved η approaching 10% in p- BaSi_2 /n-Si heterojunction solar cells^{16,17)} and recently demonstrated the operation of BaSi_2 homojunction solar cells.¹⁸⁾ A lot of studies have been carried out thus far on BaSi_2 epitaxial films grown by molecular beam epitaxy (MBE). MBE is, however, not a practical method to form films on large-area substrates. On the other hand, vacuum evaporation and sputtering are more feasible methods than MBE. BaSi_2 films formed by vacuum evaporation using BaSi_2 granules have been reported by Usami and Hara *et al.*,¹⁹⁻²²⁾ and they achieved a high carrier lifetime of 4.8 μs in the films grown at 500 °C²¹⁾ and p- BaSi_2 /n-Si heterojunction solar cells.²²⁾ Sputtering is another large-area thin-film growth technique, and has been used to form semiconducting silicides such as $\beta\text{-FeSi}_2$ and Mg_2Si .^{23,24)} Previously, we have significantly improved photoresponsivities of BaSi_2 films formed by sputtering on a Si(111) substrate at 600 °C when the sputtering pressure (P) was set to 0.25 Pa.²⁵⁾ However, the influence of the P on the photoresponse properties of BaSi_2 films has yet to be investigated. The Ba-to-Si atomic ratio of deposited films changes depending on the P during sputtering,²⁵⁾ unlike in the Mg_2Si films by sputtering.²⁴⁾ In the case of BaSi_2 films grown by MBE, the deviation of a Ba-to-Si atomic ratio from stoichiometry affects significantly their electrical and optical properties.²⁶⁾ Therefore, it is of great importance to clarify the influence of P on the properties of BaSi_2 films formed by sputtering.

In this study, we grew BaSi₂ films at difference P values in the range 0.25–1.0 Pa for the growth of 200-nm-thick BaSi₂ films at a substrate temperature of 600 °C, and studied the influence of P on their photoresponsivities. We also examined the effect of two-step growth technique for BaSi₂ films, that is, the Ba atomic ratio was set higher in the 1st step than in the 2nd step. This is to flatten the Ba-to-Si atomic ratio especially around the BaSi₂/Si interface, where the Si atomic ratio is likely to be in excess because of the diffusion of Si atoms from the Si substrate. Similar technique has been used to control the crystal orientation of BaSi₂ films grown by MBE²⁷⁾ and by vacuum evaporation,²⁸⁾ other semiconducting silicides.²⁹⁾ By using this technique, the photoresponsivity was significantly enhanced to the extent that it reaches a value as high as those of MBE-grown BaSi₂ films.

We used helicon-wave excited plasma (HWP, ULVAC MB00-1040) sputtering with a 2-inch-diameter polycrystalline stoichiometric BaSi₂ target (Tosoh). Details of the sample preparation are summarized in Table I. The deposited Ba-to-Si atomic ratio was in excess of Si when only the BaSi₂ target was sputtered.²⁵⁾ Thereby, we added three plate-like Ba sources (1.0 × 1.0 cm²) on the BaSi₂ target to achieve the formation of BaSi₂ films.²⁵⁾ In this work, first, we fabricated approximately 200-nm-thick BaSi₂ films (samples A1-A4) on a heated n-Si (111) substrate at 600 °C by sputtering. The sputtering pressure of Ar was set at 0.25, 0.4, 0.8, and 1.0 Pa, respectively, followed by a 3-nm-thick amorphous Si capping layer to prevent oxidation of the sample surface.³⁰⁾ In the second experiment, we formed BaSi₂ films (sample A5) by a two-step growth method, wherein approximately a 10-nm-thick layer was formed at 500 °C and $P = 1.0$ Pa, followed by the formation of overlayers at 600 °C and $P = 0.5$ Pa. The flow rate of Ar was set to 10 sccm, and the radio-frequency power was set to 100 W. Raman spectroscopy (JASCO NRS-5100) using a frequency-doubled neodymium-doped-yttrium–aluminum–garnet (Nd:YAG) laser (532 nm, 5.1 mW) and grazing-incidence (GI) 2 θ X-ray diffraction (XRD) with Cu-K α radiation (Rigaku SmartLab) and were used to characterize the crystalline quality of the grown layers. N⁺-type Si (111) (resistivity $\rho < 0.01$ Ω cm) substrates were used for the

photoresponsivity measurement to provide a negligible contribution of photogenerated carriers in the n^+ -Si substrate. Indium–tin oxide (ITO) surface electrodes with thicknesses of 80 nm and diameter of 1 mm and Al rear electrodes were fabricated by sputtering. The photoresponse spectra were acquired by a lock-in technique using a xenon lamp with a single monochromator with a focal length of 25 cm (Bunko Keiki SM-1700A and RU-60N). The light intensity of the lamp was calibrated using a pyroelectric sensor (Melles Griot 13PEM001/J). We used a high ρ n-type Si (111) ($\rho > 1000 \text{ } \Omega\text{cm}$) substrate for the Hall measurement. All the measurement was performed at room temperature (RT). The Ba-to-Si atomic ratio of samples deposited at RT was measured by Rutherford backscattering spectrometry (RBS).²⁵⁾

Figure 1 shows GI-XRD patterns of samples A1-A5. For reference, the calculated diffraction pattern of the orthorhombic BaSi_2 is also shown. All of the observed diffraction peaks are assigned to BaSi_2 , showing that BaSi_2 films were grown. There is not so much difference in the diffraction peaks among samples.

Figure 2 shows the Raman spectra of all these samples. The Raman lines originate from Si tetrahedra with T_h symmetry in the lattice of BaSi_2 . Identification of Raman lines is given in Ref. 31. The transverse optical phonon line of Si (Si_{TO}) was observed in samples A1 and A2, sputtered at $P = 0.25$ and 0.4 Pa , respectively. Considering that the absorption coefficient (α) of BaSi_2 at a wavelength of 532 nm is $\alpha = 3 \times 10^5 \text{ cm}^{-1}$,¹¹⁾ the penetration depth of the laser light was limited to around $1/\alpha \times 3 \sim 0.1 \text{ } \mu\text{m}$. This value is smaller than the layer thickness of BaSi_2 . Hence the Si_{TO} signal in samples A1 and A2 is interpreted to originate from crystalline Si included in the BaSi_2 film. Similar Si_{TO} signals were detected in MBE-grown BaSi_2 films when the deposited Si atomic ratio was high, being in excess of Si from stoichiometry.^{26,32)}

Figure 3(a) shows Ba (red) and Si (black) atomic ratios as a function of P for the samples deposited at RT without an additional Ba source (dotted line) and those with one Ba source on the BaSi_2 target (solid lines), measured by RBS.²⁵⁾ With decreasing P , the Si atomic

ratio is increased. Si atoms are also diffused from the heated Si substrate into the grown layer.²⁶⁾ Therefore, it is reasonable to consider that the excess Si atoms exist in the form of crystalline Si in the BaSi₂ layers when $P = 0.25$ and 0.4 Pa. Here, we discuss why the Ba-to-Si atomic ratio depends on P . Figure 3(b) shows the experimentally obtained P dependence of deposition rate of sputtered films when the substrate temperature was set at RT to prevent the diffusion of Si atoms from the Si substrate.²⁵⁾ The increase of P has both positive and negative contributions to the deposition rate due to the increase of both the sputtering yield and the scattering degree between Ar and sputtered particles. The fact that the deposition rate decreased as the P increased suggests that the latter effect appeared significant. The arrival rate, thereby the atomic ratio of sputtered films, is sensitive to the ratios of atomic numbers between the sputtered atoms (Si and Ba) and the sputtering gas molecules (Ar).³³⁾ The atomic weight between Ba, Ar, and Si is in the order $M_{\text{Ba}} \gg M_{\text{Ar}} > M_{\text{Si}}$, meaning that the effect of scattering by Ar atoms is more significant on Si atoms than Ba atoms. That's why the atomic ratio of Si decreased with increasing P in Fig. 3(a). A larger atomic ratio of Si in the low P region than stoichiometry means that the sputtering yield of Si (Y_{Si}) is more than Ba (Y_{Ba}) from a BaSi₂ target, whereas Y_{Si} is smaller than Y_{Ba} ($Y_{\text{Si}}/Y_{\text{Ba}} \sim 0.5$) as far as Si and Ba bulks are concerned.³⁴⁾ We thus speculate that it has something to do with the fact that Ba atoms in the BaSi₂ bulk exist in the form of positively charged ions, while Si tetrahedra (Si₄) are negatively charged.³⁵⁾

Figure 4(a) shows the photoresponse spectra of samples A1-A4, sputtered at various P values. The bias voltage (V_{bias}) of 0.5 V was applied to the bottom electrode with respect to the front ITO electrode to extract the photogenerated holes in the n-type BaSi₂ films into the ITO electrode. The photoresponsivities of all the samples rapidly increased with V_{bias} for photon energies larger than the band gap of BaSi₂ (~ 1.3 eV). Hence, the spectrum is derived from photogenerated carriers in the BaSi₂ films. The photoresponsivity was drastically changed depending on P , and reached a maximum of 0.29 A/W at 2.3 eV for sample A3, sputtered at $P = 0.8$ Pa. This result means that the Ba-to-Si atomic ratio of the BaSi₂ film in sample A3 is close

to stoichiometry. However, the Si atomic ratio in the sputtered film around the BaSi₂/Si interface is considered to be in excess of Si due to the diffusion of Si atoms from the Si substrate. This was confirmed in MBE-grown BaSi₂ films by RBS.²⁶⁾ According to a supercell approach based on first-principle density functional theory by Kumar *et al.*,³⁵⁾ Si vacancies are most likely to emerge in BaSi₂ regardless in a Si-rich or Ba-rich condition, generating localized states within the band gap, and degrading the photoresponsivity. We therefore attempted to decrease the Si atomic ratio in the BaSi₂ film around the BaSi₂/Si interface by a two-step growth technique, wherein the Ba atomic ratio was set higher in the 1st step ($P = 1.0$ Pa) than in the 2nd step ($P = 0.5$ Pa). Figure 4(b) shows the photoresponse spectrum of sample A5, fabricated by the two-step method, and sample A3 ($P = 0.8$ Pa). The photoresponsivity further increased in sample A5 compared to sample A3; the photoresponsivity reached 0.75 A/W at 2.0 eV at $V_{\text{bias}}=0.5$ V. This value is almost equivalent to those of BaSi₂ epitaxial films grown by MBE.²⁶⁾ We attribute this photoresponsivity enhancement to the Ba-to-Si atomic ratio in the BaSi₂ film in sample A5 being more close to stoichiometry on the whole than those in other samples. As shown in Figs. 1 and 2, we cannot see a pronounced difference in crystalline quality of BaSi₂ films between sample A5 and others. Regarding the electrical properties of grown films, there was also not so much difference between samples. The electron concentration was of the order of 10^{16} cm⁻³ at RT and the mobility was in the range 900–1000 cm²/Vs, similar to undoped n-BaSi₂ epitaxial films grown by MBE.⁹⁾ We speculate that small barrier heights at grain boundaries (GBs) in BaSi₂³⁶⁾ may not deteriorate the electron transport across GBs, resulting in such a large mobility even in polycrystalline BaSi₂ films. On the basis of these results, we conclude that sputtering is a promising fabrication method for BaSi₂ films.

In summary, we formed 200-nm-thick BaSi₂ films on Si(111) substrates by sputtering and investigated the influence of deposition pressure on their photoresponsivities. The photoresponsivity changed significantly on P as observed in those by MBE, and reached a maximum of 0.29 A/W at 2.3 eV at $V_{\text{bias}} = 0.5$ V when $P = 0.8$ Pa. The photoresponsivity was

further increased in BaSi₂ films prepared by a two-step growth technique; increasing up to 0.75 A/W at 2.0 eV at $V_{\text{bias}} = 0.5$ V. This value was equivalent to those of BaSi₂ epitaxial films by MBE.

Acknowledgments

This study was financially supported by JSPS KAKENHI Grant Numbers 17K18865 and 18H03767 and JST MIRAI.

- 161 1) K. Yoshikawa, H. Kawasaki, W. Yoshida, T. Irie, K. Konishi, K. Nakano, T. Uto, D. Adachi,
162 M. Kanematsu, H. Uzu, and K. Yamamoto, *Nat. Energy* **2**, 17032 (2017).
- 163 2) W. Shockley and H. J. Queisser, *J. Appl. Phys.* **32**, 510 (1961).
- 164 3) P. Jackson, R. Wuerz, D. Hariskos, E. Lotter, W. Witte, and M. Powalla, *Phys. Status Solidi*
165 *RL* **10**, 583 (2016).
- 166 4) X. Wu, *Sol. Energy* **77**, 803 (2004).
- 167 5) J. Burschka, N. Pellet, S.-J. Moon, R. Humphry-Baker, P. Gao, M. K. Nazeeruddin, and M.
168 Grätzel, *Nature* **499**, 316 (2013).
- 169 6) W. S. Yang, J. H. Noh, N. J. Jeon, Y. C. Kim, S. Ryu, J. Seo, and S. I. Seok, *Science* **348**,
170 1234 (2015).
- 171 7) T. Suemasu, *Jpn. J. Appl. Phys.* **54**, 07JA01 (2015).
- 172 8) T. Suemasu and N. Usami, *J. Phys. D: Appl. Phys.* **50**, 023001 (2017).
- 173 9) K. Morita, Y. Inomata, and T. Suemasu, *Thin Solid Films* **508**, 363 (2006).
- 174 10) D. B. Migas, V. L. Shaposhnikov, and V. E. Borisenko, *Phys. Status Solidi B* **244**, 2611
175 (2007).
- 176 11) K. Toh, T. Saito, and T. Suemasu, *Jpn. J. Appl. Phys.* **50**, 068001 (2011).
- 177 12) M. Kumar, N. Umezawa, and M. Imai, *Appl. Phys. Express* **7**, 071203 (2014).
- 178 13) M. Baba, M. Kohyama, and T. Suemasu, *J. Appl. Phys.* **120**, 085311 (2016).
- 179 14) K. O. Hara, N. Usami, K. Toh, M. Baba, K. Toko, and T. Suemasu, *J. Appl. Phys.* **112**,
180 083108 (2012).
- 181 15) K. O. Hara, N. Usami, K. Nakamura, R. Takabe, M. Baba, K. Toko, and T. Suemasu, *Appl.*
182 *Phys. Express* **6**, 112302 (2013).
- 183 16) S. Yachi, R. Takabe, K. Toko, and T. Suemasu, *Appl. Phys. Lett.* **109**, 072103 (2016).
- 184 17) T. Deng, T. Sato, Z. Xu, R. Takabe, S. Yachi, Y. Yamashita, K. Toko, and T. Suemasu, *Appl.*
185 *Phys. Express* **11**, 062301 (2018).
- 186 18) K. Kodama, K. Toko, and T. Suemasu, *Jpn. J. Appl. Phys.* **57**, 050310 (2018).
- 187 19) K. O. Hara, Y. Nakagawa, T. Suemasu, and N. Usami, *J. Appl. Phys.* **54**, 07JE02 (2015).
- 188 20) K. O. Hara, C. T. Trinh, K. Arimoto, J. Yamanaka, K. Nakagawa, Y. Kurokawa, T.
189 Suemasu, and N. Usami, *J. Appl. Phys.* **120**, 045103 (2016).
- 190 21) C. T. Trinh, Y. Nakagawa, K. O. Hara, R. Takabe, T. Suemasu, and N. Usami, *Mater. Res.*
191 *Express* **3**, 076204 (2016).
- 192 22) K. Takahashi, Y. Nakagawa, K. O. Hara, I. Takahashi, Y. Kurokawa, and N. Usami, *MRS*
193 *Adv.* **3**, 1435 (2018).
- 194

- 23) T. Yoshitake, A. Yuri, and K. Nagayama, *Appl. Phys. Lett.* **88**, 182104 (2006).
- 24) S. Ogawa, A. Katagiri, T. Shimizu, M. Matsushima, K. Akiyama, Y. Kimura, H. Uchida, and H. Funakubo, *J. Electron. Mater.* **43**, 2269 (2014).
- 25) S. Matsuno, R. Takabe, S. Yokoyama, K. Toko, M. Mesuda, H. Kuramochi, and T. Suemasu, *Appl. Phys. Express* **11**, 071401 (2018).
- 26) R. Takabe, T. Deng, K. Kodama, Y. Yamashita, T. Sato, K. Toko, and T. Suemasu, *J. Appl. Phys.* **123**, 045703 (2018).
- 27) Y. Inomata, T. Nakamura, T. Suemasu, and F. Hasegawa, *Jpn. J. Appl. Phys.* **43**, L478 (2004).
- 28) K. O. Hara, C. T. Cham, Y. Kurokawa, K. Arimoto, J. Yamanaka, K. Nakagawa, and N. Usami, *Thin Solid Films* **636**, 546 (2017).
- 29) N. Hiroi, T. Suemasu, K. Takakura, N. Seki, and F. Hasegawa, *Jpn. J. Appl. Phys.* **40**, L1008 (2001).
- 30) R. Takabe, W. Du, K. Ito, H. Takeuchi, K. Toko, S. Ueda, A. Kimura, and T. Suemasu, *J. Appl. Phys.* **119**, 025306 (2016).
- 31) H. Hoshida, N. Murakoso, T. Suemasu, and Y. Terai, *Defect and Diffusion Forum* **386**, 43 (2018).
- 32) Y. Terai, H. Yamaguchi, H. Tsukamoto, N. Murakoso, M. Iinuma, and T. Suemasu, *Jpn. J. Appl. Phys.* **56**, 05DD02 (2017).
- 33) T. Motohiro and Y. Taga, *Thin Solid Films* **112**, 161 (1984).
- 34) Ar sputter yield values from National Physics Laboratory, UK.
(http://www.npl.co.uk/upload/pdf/energy_density_sublim.pdf)
- 35) M. Kumar, N. Umezawa, W. Zhou, and M. Imai, *J. Mater. Chem. A* **5**, 25293 (2017).
- 36) D. Tsukahara, M. Baba, S. Honda, Y. Imai, K. O. Hara, N. Usami, K. Toko, J. H. Werner, and T. Suemasu, *J. Appl. Phys.* **116**, 123709 (2014).

221 Table I. Sample preparation detail; pressure (P), substrate temperature (T_s) during the sputtering,
 222 layer thickness (d), the number of plate-like Ba source on the target (N) are specified.

	P	T_s	d	N
Sample	(Pa)	(°C)	(nm)	
A1	0.25	600	272	3
A2	0.4	600	230	3
A3	0.8	600	235	3
A4	1.0	600	220	3
A5	0.5/1.0	500/600	300	3

223

224

Fig. 1 GI-XRD patterns of samples A1-A6, sputtered at 600 °C on Si(111) substrates.

Fig. 2 Raman spectra of samples A1-A6, sputtered at 600 °C on Si(111) substrates.

Fig. 3 (a) Ba (red) and Si (black) atomic ratios as a function of P for the samples prepared without (dotted lines) and with one Ba source on the BaSi₂ target (solid lines). The broken lines are plotted as guides showing the Ba and Si atomic ratios of the BaSi₂ target. (b) Dependence of deposition rate of films sputtered at RT when only the BaSi₂ target is used. (a) and (b) are reproduced from Ref. 25.

Fig. 4 Photoresponse spectra of (a) samples A1-A4 and (b) samples A3 (one-step growth) and A5 (two-step growth), under $V_{\text{bias}} = 0.5$ V applied between the top and bottom electrodes.

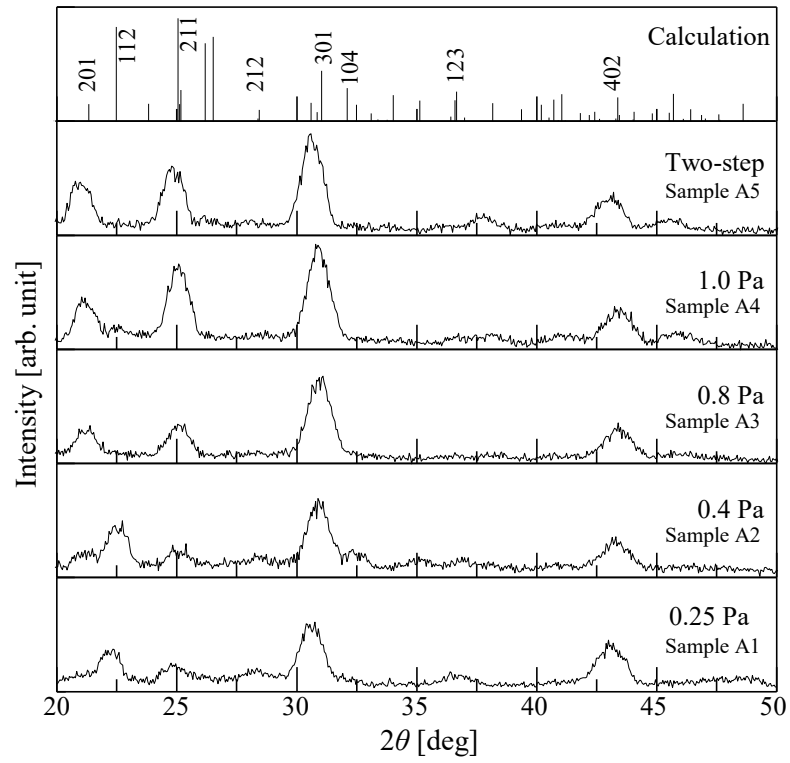


Fig. 1

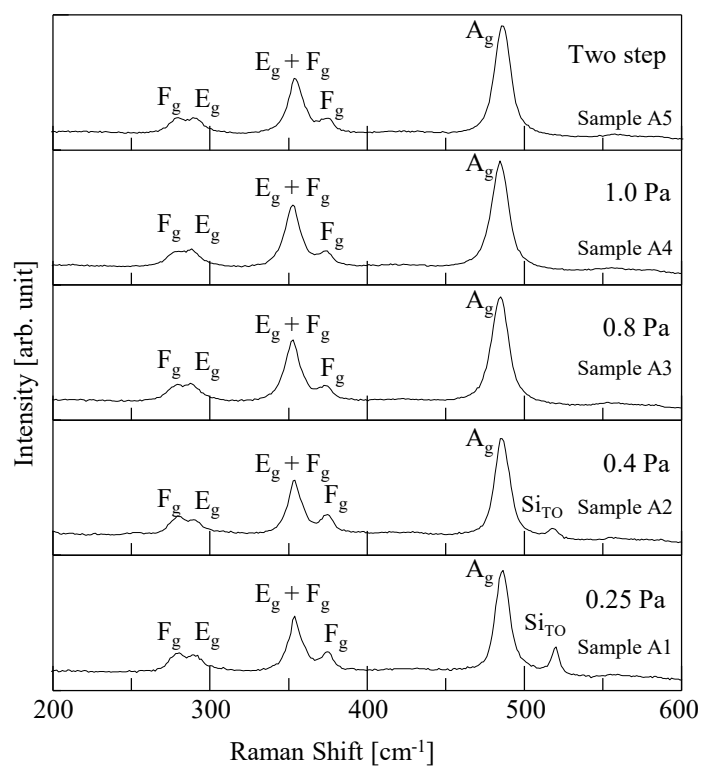


Fig. 2

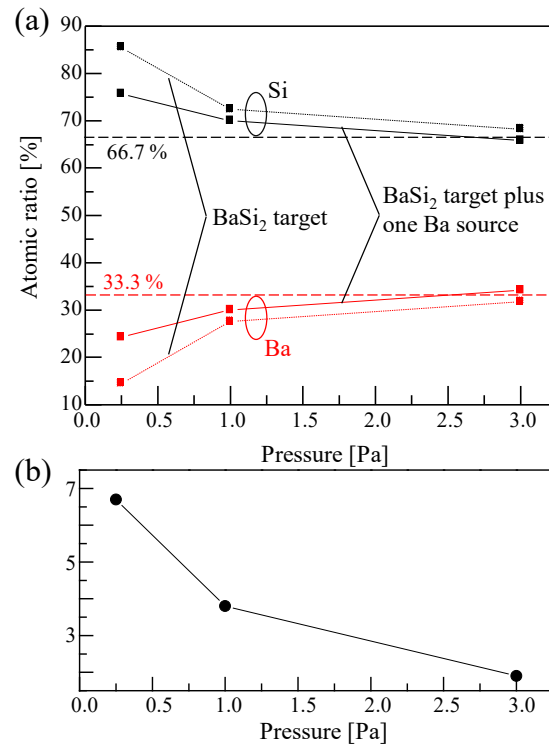


Fig. 3

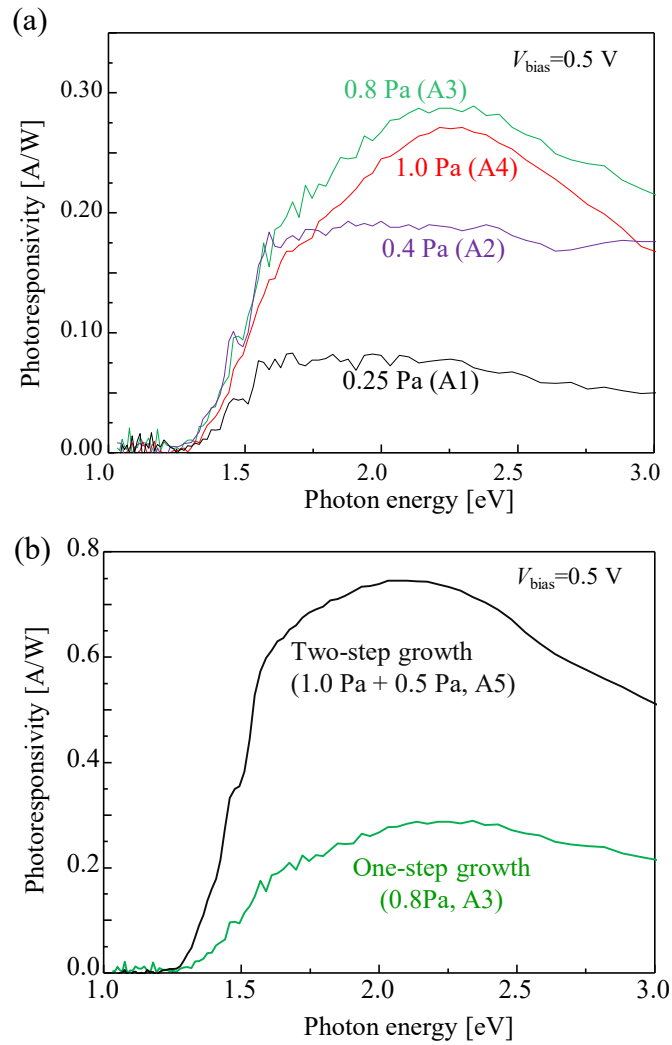


Fig. 4